J. Fluid Mech. (2005), *vol.* 541, *pp.* 55–64.
doi:10.1017/S0022112005006130 Printed in the United Kingdom

Exact solutions of the Navier–Stokes equations having steady vortex structures

By M. Z. BAZANT[1] AND H. K. MOFFATT[2]

[1]Department of Mathematics, Massachusetts Institute of Technology, Cambridge, MA 02139, USA

[2]Department of Applied Mathematics and Theoretical Physics, Cambridge University, Wilberforce Road, Cambridge CB3 0WA, UK

(Received 18 April 2005 and in revised form 25 June 2005)

We present two classes of exact solutions of the Navier–Stokes equations, which describe steady vortex structures with two-dimensional symmetry in an infinite fluid. The first is a class of similarity solutions obtained by conformal mapping of the Burgers vortex sheet to produce wavy sheets, stars, flowers and other vorticity patterns. The second is a class of non-similarity solutions obtained by continuation and mapping of the classical solution to steady advection–diffusion around a finite circular absorber in a two-dimensional potential flow, resulting in more complicated vortex structures that we describe as avenues, fishbones, wheels, eyes and butterflies. These solutions exhibit a transition from 'clouds' to 'wakes' of vorticity in the transverse flow with increasing Reynolds number. Our solutions provide useful test cases for numerical simulations, and some may be observable in experiments, although we expect instabilities at high Reynolds number. For example, vortex avenues may be related to counter-rotating vortex pairs in transverse jets, and they may provide a practical means to extend jets from dilution holes, fuel injectors, and smokestacks into crossflows.

1. Introduction

There are very few known exact solutions of the Navier–Stokes equations of viscous fluid dynamics, which have the familiar dimensionless form:

$$\frac{\partial \boldsymbol{u}}{\partial t} + \boldsymbol{u}\cdot\nabla\boldsymbol{u} = -\nabla p + Re^{-1}\nabla^2\boldsymbol{u}, \tag{1.1}$$

$$\nabla\cdot\boldsymbol{u} = 0. \tag{1.2}$$

In this paper, we shall construct new families of steady solutions, for which pressure, and inertial and viscous stresses are in equilibrium, implying a corresponding balance between advection and diffusion of vorticity.

This balance is nicely illustrated by the *vortex sheet* (Burgers 1948) shown in figure 1, which is one of the least trivial known solutions to equations (1.1)–(1.2). A steady two-dimensional vortex structure is formed when the vorticity between two shearing half-planes of fluid moving in opposite directions is confined by a transverse potential flow with uniform strain rate. The dependence on the Reynolds number is quite simple, since this only sets the $O(Re^{-1/2})$ scale of the thickness of the vortex sheet, but not its spatial structure, which is self-similar.

Burgers' solution has been extended to allow for a time-dependent (but spatially uniform) transverse strain rate (Gibbon, Fokas & Doering 1999); here by contrast, we focus on the geometrical complexity of steady vortex structures maintained by

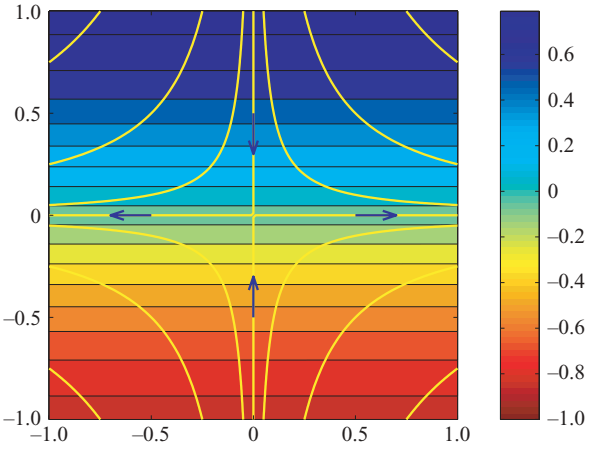

FIGURE 1. The Burgers vortex sheet. Colour contours are contours of the out-of-plane velocity component (and also vortex lines of the flow); the yellow streamlines are those of the in-plane velocity field. Note that the same colour scale applies to all subsequent figures.

non-uniform strain. We apply a conformal-mapping technique, briefly explained in § 2, to two different base states. A first class of new steady solutions is obtained in § 3 by conformal mapping of the Burgers vortex sheet to produce wavy sheets, flowers, stars, and other vorticity patterns. A second class is derived in § 4 starting from the classical problem of advection–diffusion of an absorbing cylinder in a uniform background flow, to produce what may be described as vortex avenues† (the two-dimensional analogue of vortex tubes), fishbones, wheels, eyes, and butterflies. We conclude in § 5 with a discussion of possible applications of our solutions.

2. Background

We seek steady solutions with two-dimensional symmetry of the form

$$\boldsymbol{u}(x, y, z) = (\nabla\phi(x, y), v(x, y)), \tag{2.1}$$

where ϕ is the velocity potential for the flow in the (x, y)-plane and v is the out-of-plane velocity component. The vorticity field is

$$\boldsymbol{\omega} = (\partial v/\partial y, -\partial v/\partial x, 0), \tag{2.2}$$

so that the contours $v = \text{const.}$ are also the vortex lines of the flow. Substituting equation (2.1) into the Navier–Stokes equations yields

$$\nabla^2\phi = 0, \tag{2.3}$$

$$Re\nabla\phi \cdot \nabla v = \nabla^2 v, \tag{2.4}$$

$$p = -(1/2)|\nabla\phi|^2. \tag{2.5}$$

The first two equations (2.3)–(2.4) are those of steady advection–diffusion of a scalar v in a two-dimensional potential flow, where Re plays the role of the Péclet number, so the out-of-plane velocity is thus determined entirely by a balance between inertia and viscosity. The third equation (2.5) determines the dynamical pressure p as (minus) the

† A vortex avenue is a type of mixing-layer, non-uniform in the direction of the vorticity field within the layer; it should not of course be confused with a vortex street!

in-plane kinetic energy density since it comes from a balance between pressure and inertia (Bernoulli's law).

The classical vortex sheet of Burgers (1948),

$$\phi = x^2 - y^2, \quad v = \mathrm{erf}\left(Re^{1/2}y\right), \quad p = -2(x^2 + y^2), \tag{2.6}$$

provides the simplest solution of the form (2.1), but this is by no means the only one. The reason is that the system of advection–diffusion equations (2.3)–(2.4) is in a conformally invariant class (Bazant 2004), so that we can apply conformal mapping techniques to generate new solutions. One manifestation of conformal invariance is the classical transformation to streamline coordinates (Boussinesq 1905), which is simply mapping to a domain of uniform flow. Although often used to analyse high-Reynolds-number flows (Eames & Bush 1999; Hunt & Eames 2002), streamline coordinates are not directly useful here, since they introduce unphysical branch cuts in the flow (which would correspond to inviscid slipping boundaries) emanating from stagnation points; we can, however, still exploit the general idea of conformal mapping.

3. Similarity solutions: vortex sheets, stars and flowers

Consider a conformal mapping $w = f(z)$ from the z-plane containing some new solution, to the w-plane containing the Burgers vortex sheet. From (2.6), the transformed solution is then of the form

$$\phi = Re\,[f(z)]^2, \quad v = \mathrm{erf}\left(Re^{1/2}\mathrm{Im}\,f(z)\right), \quad p = -2|f'(z)f(z)|^2. \tag{3.1}$$

The in-plane velocity is constructed in the usual way, $\nabla\phi = 2\overline{f'(z)f(z)}$, where we now represent in-plane vectors by complex scalars. The vorticity is given by

$$\boldsymbol{\omega} = 2(Re/\pi)^{1/2}\overline{f'(z)}\exp\left(-Re[\mathrm{Im}\,f(z)]^2\right), \tag{3.2}$$

and the shear-strain rate by $\nabla v = \mathrm{i}\boldsymbol{\omega}$. For different choices of $f(z)$, the vortex lines can have rather complicated spatial structures.

If the flow is to be free of singularities, then $f(z)$ must be entire (analytic everywhere). In that case, Liouville's theorem states that a non-constant $f(z)$ must also be unbounded. Apart from the trivial case of stretching and translating Burgers' vortex sheet by a linear $f(z)$, this implies the existence of powers z^k, $k \geqslant 2$, in the Taylor series (valid everywhere), which dominate as $|z| \to \infty$, so the map must be multivalent (not one-to-one). By the Minimum Modulus Principle applied to $f'(z)$, this further implies the existence of (isolated) points where the mapping loses conformality, $f'(z) = 0$, at stagnation points of the transverse flow.

We conclude that all non-trivial new solutions in the class (3.1) which are free of singularities involve a patchwork of multiple warped copies of Burgers' vortex sheet. This general result is illustrated by the simple mappings, $f(z) = z^n$ ($n = 2, 3, \ldots$), which produce $2n$-pointed *vortex stars*, as illustrated in figure 2(*a*) for the case $n = 3$. Entire functions with multiple roots, where $f(z) = 0$, introduce additional images of the stagnation point in Burgers' vortex sheet. The case $f(z) = 1 - z^2$, shown in figure 2(*b*), has three stagnation points (since $f'(0) = f(\pm 1) = 0$), but looks like a four-pointed star, or *vortex cross*, far away (since $f(z) \sim -z^2$ as $|z| \to \infty$).

More generally, we may construct physical solutions by allowing $f(z)$ to be any meromorphic function (with only pole singularities). A simple class of solutions with only one singularity is obtained by Möbius transformations, which effectively move the quadrupole singularity at infinity in Burgers' solution to a finite point in the plane. If the pole of the inverse map does not lie on the real axis, then the solution

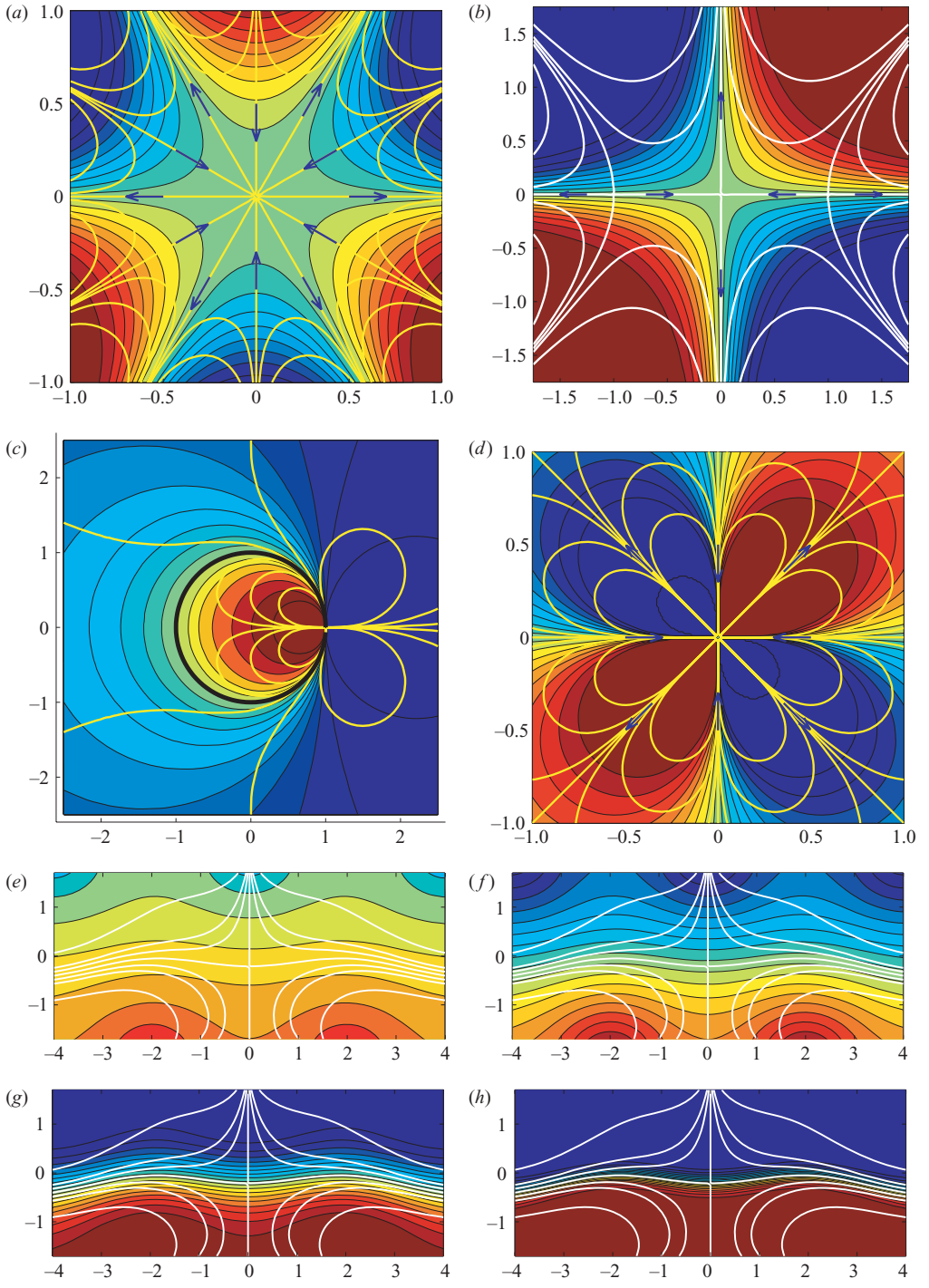

FIGURE 2. Solutions obtained by conformal mapping, $w = f(z)$, to Burgers' vortex sheet: (*a*) a vortex star, $f(z) = z^3$; (*b*) a vortex cross with stagnation points on its arms, $f(z) = 1 - z^2$; (*c*) a circular vortex sheet, $f(z) = (1+z)/\mathrm{i}(1-z)$ (where the black circle indicates the separatrix of the transverse flow); (*d*) a vortex flower, $f(z) = z^{-2}$; and (*e–h*) wavy vortex sheets, non-uniformly strained by dipole singularities, $f(z) = z + \sum_{j=1}^{3}(z - z_j)^{-1}$, $z_1 = 2.5\mathrm{i}$, $z_2 = 2 - 2.5\mathrm{i}$, $z_3 = -2 - 2.5\mathrm{i}$, for (*e*) $Re = 0.01$, (*f*) $Re = 0.1$, (*g*) $Re = 1$, and (*h*) $Re = 10$.

corresponds to a *circular vortex sheet*, because the centre of the Burgers vortex sheet is mapped to a circle, as shown in figure 2(*c*). If the pole lies on the real axis, then the quadrupole separates two regions of opposite out-of-plane flow. This solution is easily generalized to a *vortex flower* with $2n$ 'petals', given by the multivalent mapping, $f(z) = z^{-n}$ $(n = 1, 2, \ldots)$. In this case, the vorticity between the petals is confined by a $4n$-pole singularity in the in-plane flow, located at the centre of the flower, as shown in figure 2(*d*).

By placing singularities in the transverse potential flow, non-uniform strain may be applied to Burgers' vortex sheet, without changing its basic topology. For example, we may place dipole singularities in the low-shear regions of nearly uniform out-of-plane velocity with maps of the form, $f(z) = z + \sum_j a_j (z - z_j)^{-1}$. A case with three dipole singularities, one above and two below the sheet, is shown in figure 2(*e–h*) for different values of *Re*. Since the map introduces some length scales, the spatial structure of the solution has a more complicated dependence on *Re*, which is not simply a rescaling of the Cartesian coordinate system, as in the scale-free examples of figures 2(*a*) and 2(*d*). Nevertheless, as illustrated in figure 2(*e–h*), the geometry of the vortex lines (constant v) and the shear-strain-rate lines (∇v) is independent of *Re*, since it depends only on the conformal map. Changing *Re* simply changes the magnitude of v along the same set of iso-velocity lines, but not the direction of ∇v. This is a consequence of a general equivalence theorem for conformally invariant fields (Bazant 2004). The present case of advection–diffusion in a potential flow was first discussed by Koplik, Redner & Hinch (1994).

As this example illustrates, the vortex structures obtained above from Burgers' solution have a relatively simple dependence on the Reynolds number, which can be removed by rescaling the curvilinear coordinates, $f(z) \mapsto Re^{1/2} f(z)$. They are 'similarity solutions' in the sense that v depends on only one curvilinear coordinate (Bazant 2004). Solutions with a more complicated spatial dependence on the Reynolds number can be obtained from other classical solutions to the advection–diffusion problem, equations (2.3)–(2.4).

4. Non-similarity solutions: vortex avenues, fishbones, and wheels

To construct more complicated solutions to the Navier–Stokes equations, we start with the canonical problem of steady advection–diffusion around an absorbing, circular cylinder in a uniform background flow of constant velocity and constant concentration (Choi *et al.* 2004):

$$Pe\, \nabla\phi \cdot \nabla c = \nabla^2 c \quad \text{and} \quad \nabla^2 \phi = 0 \quad \text{for} \quad |z| > 1, \tag{4.1}$$

$$c = 0, \quad \hat{\boldsymbol{n}} \cdot \nabla\phi = 0 \quad \text{for} \quad |z| = 1 \quad \text{and} \quad c \to 1, \quad \nabla\phi \to \hat{\boldsymbol{x}} \quad \text{as} \quad |z| \to \infty. \tag{4.2}$$

The harmonic velocity potential for flow past a cylinder is

$$\phi(z) = Re\, \Phi(z), \quad \Phi(z) = z + z^{-1}. \tag{4.3}$$

The (non-harmonic) solution for the concentration, $c(z, \bar{z}, Pe)$, is more complicated, but it has been described in the literature on the mathematical theory of freezing (van Wijngaarden 1966; Maksimov 1976; Kornev & Mukhamadullina 1994; Choi *et al.* 2004).

Let us briefly describe this particular solution to the advection–diffusion problem, equations (4.1)–(4.2). It is convenient to change variables, $\tilde{c}(\tilde{x}, \tilde{y}) = 1 - c(z, \bar{z}, Pe)$ to streamline coordinates, $\tilde{x} + \mathrm{i}\tilde{y} = (z + z^{-1})/2$, where the disk is mapped to a finite strip

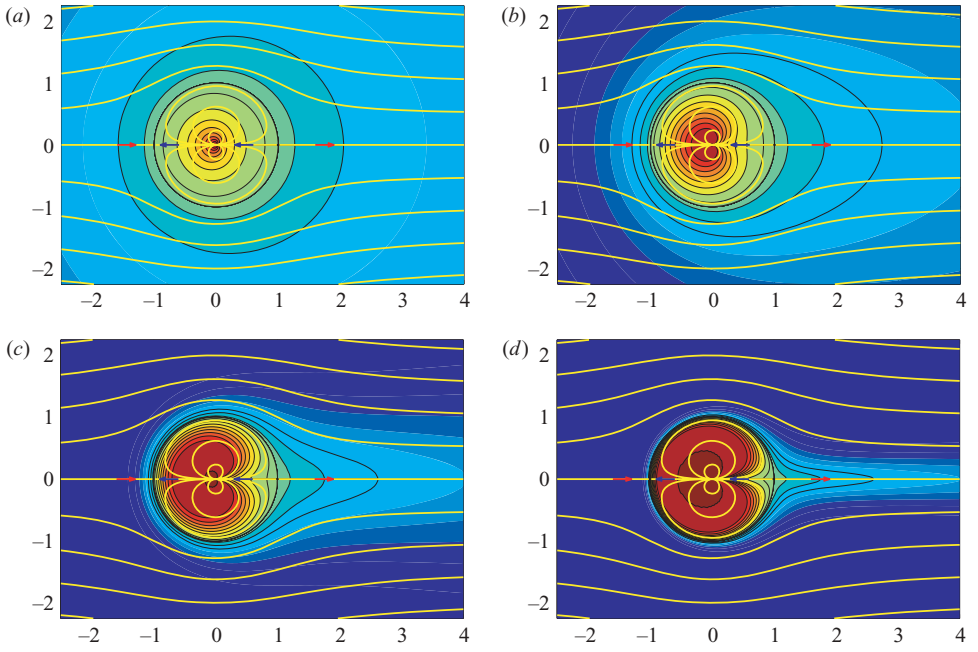

FIGURE 3. Steady vortex avenues confined by transverse flow with a dipole source inside and a uniform background flow outside (a dipole at ∞). These transverse jets exhibit a non-trivial dependence on the Reynolds number with a transition from 'clouds' to 'wakes' of vorticity: (*a*) $Re = 0.1$, (*b*) $Re = 1$, (*c*) $Re = 10$, (*d*) $Re = 100$.

on the real axis, $-1 \leqslant \tilde{x} \leqslant 1$. The solution can then be expressed as a convolution

$$\tilde{c}(\tilde{x}, \tilde{y}) = 2 \int_{-1}^{1} G(\tilde{x} - \tilde{x}', \tilde{y}) \sigma(\tilde{x}') \, \mathrm{d}\tilde{x}', \tag{4.4}$$

in terms of the Green function,

$$G(\tilde{x}, \tilde{y}) = \mathrm{e}^{Pe\tilde{x}} K_0(Pe \sqrt{\tilde{x}^2 + \tilde{y}^2})/2\pi, \tag{4.5}$$

where $K_0(\tilde{r})$ is a modified Bessel function of the second kind, and the function $\sigma(\tilde{x})$, the flux density along the strip, satisfies the following integral equation (Pearson 1957):

$$\int_{-1}^{1} \mathrm{e}^{Pe(\tilde{x}-\tilde{x}')} K_0(Pe|\tilde{x} - \tilde{x}'|) \sigma(\tilde{x}') \, \mathrm{d}\tilde{x}' = \pi, \quad -1 < \tilde{x} < 1. \tag{4.6}$$

This equation cannot be solved in terms of elementary functions, but very accurate uniformly valid approximations and numerical solutions are available (Choi *et al.* 2004)†. We may therefore regard $\sigma(\tilde{x}; Pe)$ as a 'known' special function, from which to construct exact solutions to the Navier–Stokes equations.

The advection–diffusion solution, (ϕ, c), described above is valid outside the unit disk, $|z| > 1$, but we can continue it to the inside, in order to construct a solution to the Navier–Stokes equations valid everywhere, as shown in figure 3. The complex potential for the in-plane velocity, equation (4.3), can be analytically continued everywhere, except for the flow dipole at the origin. The out-of-plane velocity can be obtained by taking advantage of symmetries. The idea is to patch together the

† Matlab scripts for numerical solutions are available at http://advection–diffusion.net.

solution outside the disk with its image under inversion, inside the disk:

$$v(z,\bar{z},Re)=\begin{cases} c(z,\bar{z},Re) & \text{if } |z|\geqslant 1 \\ -c(z^{-1},\bar{z}^{-1},Re) & \text{if } |z|<1. \end{cases} \tag{4.7}$$

Because the potential has the same symmetry, $\Phi(z^{-1})=\Phi(z)$, the fields, (ϕ, v), for $0<|z|<1$ are obtained in equations (4.3)–(4.7) by a conformal change of variables, $z\mapsto z^{-1}$, and a sign change, $c\mapsto -c$, from a solution valid in $|z|>1$. The conformal invariance of the system (4.1) and its linearity in c then imply that (ϕ, v) is a valid solution for all $|z|\neq 0, 1$.

At $z=0$ there is an in-plane dipole singularity and a constant out-of-plane velocity $v=-1$, but we must check that (ϕ, v) in equations (4.3)–(4.7) satisfies equations (2.3)–(2.4) on the unit circle, $|z|=1$. The outer solution is reflection symmetric, since $\phi(\bar{z})=\phi(z)$ and $c(\bar{z}, z, Pe)=c(z,\bar{z}, Pe)$, so the conformal mapping $z\mapsto z^{-1}$ yields the same solution inside the disk as the non-conformal mapping $z\mapsto \bar{z}^{-1}$ (sometimes called 'circular inversion'; see Needham 1997). The construction $c\mapsto -c$ as $z\mapsto\bar{z}^{-1}$ in equation (4.7) makes v locally an 'odd function' in the radial coordinate at the circle. Since $c=0$ on $|z|=1$, this implies that v and ∇v are continuous across $|z|=1$. Since ϕ and $\nabla\phi$ are also continuous (by the analyticity of Φ), the left-hand side of (2.4) is continuous across $|z|=1$. The boundary condition (4.2) implies that $\nabla^2 c\propto \nabla\phi\cdot\nabla c\to 0$ as $|z|\to 1^+$, which shows that the right-hand side of (2.4) is also continuous across $|z|=1$. This completes the proof that the vorticity field given by equations (4.3)–(4.7) does indeed provide a valid solution to the Navier–Stokes equations.

Unlike the similarity solution in figure 2(*c*) for a circular vortex sheet emanating from a flow quadrupole, this *vortex avenue*, shown in figure 3, is confined by a separate dipole inside at $z=0$ and an opposing uniform flow (dipole at ∞) outside at $z=\infty$. As discussed below, a vortex avenue is the special case of a steady transverse jet in a cross-flow. It has a non-trivial dependence on Re, inherited from the dependence of c on Pe. For $Re\ll 1$, the region of vorticity appears spread out like a 'cloud' over most of the space. For $Re\gg 1$, the vorticity is confined to an avenue of width $O(Re^{-1/2})$, which separates at the rear stagnation point to form a thin 'wake' of vorticity in the transverse flow of width also $O(Re^{-1/2})$ and length $O(1)$. The transition from clouds to wakes occurs at $Re\approx 60$ (Choi *et al.* 2004).

With an exact solution now available, it is straightforward to generate others by conformal mapping, $w=f(z)$, as we did with Burgers' vortex sheet. The new class of solutions (ϕ, v, p) is given by

$$\phi(z)=Re\,\Phi(z),\quad \Phi(z)=f(z)+f(z)^{-1}, \tag{4.8}$$

$$v(z,\bar{z},Re)=\begin{cases} c(f(z),\overline{f(z)},Re) & \text{if } |f(z)|\geqslant 1 \\ -c(f(z)^{-1},\overline{f(z)}^{-1},Re) & \text{if} |f(z)|<1, \end{cases} \tag{4.9}$$

$$p=-\tfrac{1}{2}|f'(z)|^2(1-f(z)^{-2})(1-\overline{f(z)}^{-2}). \tag{4.10}$$

For example, general Möbius transformations, $f(z)=(az+b)/(cz+d)$, produce a circular (or flat) vortex sheet confined between transverse dipoles. If the half-plane is mapped to the interior of the unit disk, the solution consists of a pair of avenues, stabilized by either diverging or converging dipoles, which resemble *vortex eyes* or a *vortex butterfly*, respectively, as shown in figures 4(*a*) and 4(*b*). The solutions illustrate how oppositely directed parallel jets can be stabilized by transverse flows.

Of course, there is no limit to the variety of solutions that may be obtained by different choices of conformal mappings $f(z)$ in equations (4.8)–(4.10). In addition to

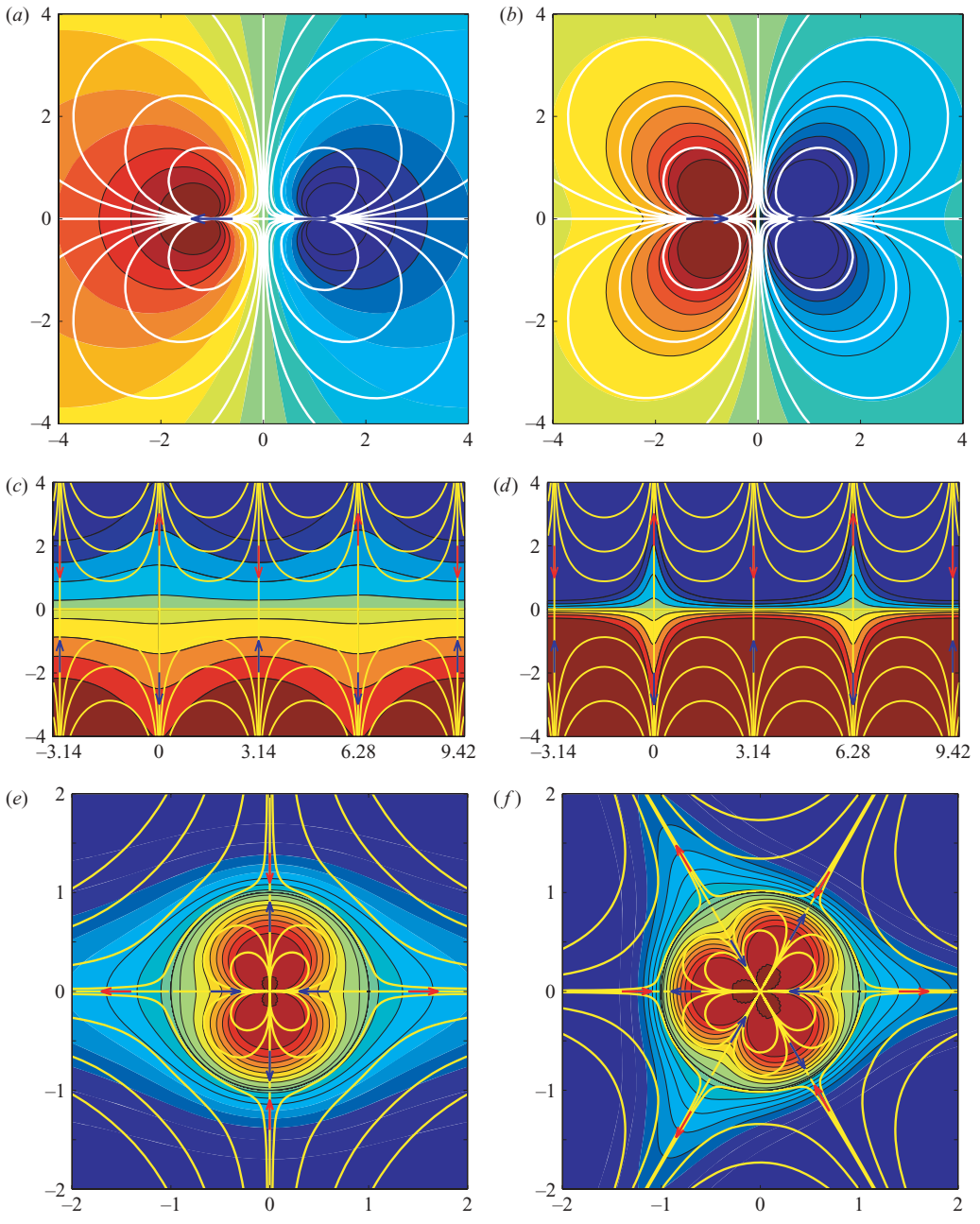

FIGURE 4. Solutions obtained by conformal mappings, $w = f(z)$, to the vortex avenues in figure 3: (*a*) vortex eyes, $f(z) = (1 + z)/(1 - z)$, a pair of avenues stabilized by transverse diverging dipoles at $Re = 1$; (*b*) a vortex butterfly, $f(z) = -(1 + z)/(1 - z)$, stabilized by converging dipoles at $Re = 10$; vortex fishbones, $f(z) = \mathrm{i} \log z$, at (*c*) $Re = 0.1$ and (*d*) $Re = 10$; and vortex wheels, (*e*) $f(z) = z^2$ and (*f*) $f(z) = z^3$, at $Re = 1$.

placing pole singularities in the fluid as before, we can also consider non-meromorphic functions, which exploit the symmetry of the solution. For example, $f(z) = \mathrm{i} \log(z)$ maps the vortex avenues in figure 3 to *vortex fishbones*, with an array of rib-like sheets connected by a transverse spine. These solutions, shown in figure 4(*c*, *d*), are

noteworthy in that they are free from singularities, like Burgers' vortex sheet, and yet they are not similarity solutions and have a complicated dependence on the Reynolds number. Mapping these solutions again with an exponential mapping of a different period to give $f(z)=z^n$, we obtain another class of vortex avenues, now confined by higher-order multipoles in the transverse flow. As the Reynolds number is increased, these solutions begin to look like *vortex wheels* with thin 'spokes' of vorticity, as shown in figure 4(e, f).

5. Discussion

We have presented two classes of exact solutions of the Navier–Stokes equations representing steady vortex structures with two-dimensional symmetry, confined by transverse potential flows. These solutions provide mathematical insights into the Navier–Stokes equations and physical insights into ways that vorticity may be confined. They also provide stringent tests for the accuracy of numerical simulations.

Our solutions are likely to be difficult to observe in the laboratory because they involve carefully placed singularities and/or stagnation points in the in-plane potential flow field, which must be achieved while also setting the appropriate out-of-plane shearing flow, which provides the vorticity. Perhaps the most promising examples to pursue in experiments would be the vortex avenues in figure 3 or the eyes and butterflies in figure 4; at high Reynolds numbers, such flows are likely to be subject to three-dimensional instability leading to turbulence, but something resembling an exact steady solution may be observable before such instability develops.

Vortex avenues may have relevance for jets in cross-flows, as produced by dilution holes of gas turbine combustors, fuel injectors, and smokestacks. Transverse jets have been studied extensively in experiments (Kamotani & Greber 1972; Fearn & Weston 1974; Smith & Mungal 1998; Su & Mungal 2004) and numerical simulations (Yuan & Street 1998; Cortelezzi & Karagozian 2001; Muppidi & Mahesh 2005*a*). A robust feature is the formation of a counter-rotating vortex pair (CVP) thought to be initiated either in the inlet pipe (Coelho & Hunt 1989) or the shear layer emanating from the orifice (Kelso, Lim & Perry 1996). Recently, Muppidi & Mahesh (2005*b*) have shown that the CVP also forms in a two-dimensional model, starting from a uniform round jet in a transverse potential flow ($Re > 1000$). Their simulations produce steadily translating jets, which resemble vortex avenues (in the moving frame), suggesting that CVP formation is influenced by the existence of an exact solution having similar steady vortex structure.

The steady vortex avenue also suggests a practical means to extend a transverse jet by introducing a CVP in a round inlet pipe. Shear layers near the walls make it difficult to reproduce the exact solution, but tuning the strength of an inlet CVP may straighten the jet trajectory or even cause it to bend upstream (prior to instability and turbulence). This design principle could be useful in controlling pollutant release from smokestacks and fuel/dilutant injection in combustors. Similarly, vortex eyes and butterflies may motivate designs with multiple inlet pipes.

Our solutions also provide possible starting points for further analysis of the Navier–Stokes equations and pose intriguing questions of linear and nonlinear stability. We have provided several classes of solutions which are completely free of singularities, obtained with arbitrary entire functions $f(z)$ in either equation (3.1) or equations (4.8)–(4.10). It would be interesting to study whether three-dimensional perturbations of these solutions remain smooth for all times, particularly in the latter case. The long, thin wakes of vorticity may be highly unstable at high Reynolds number.

M. Z. B. acknowledges the support of the Ecole Supérieure de Physique et de Chimie Industrielles through his tenure of the Chaire Paris Sciences (2002/3). H. K. M. acknowledges the support of the Fondation de l'Ecole Normale Supérieure through his tenure of the Chaire Internationale de Recherche Blaise Pascal (2001–2003), and of the Leverhulme Trust for an Emeritus Professorship (2004/5). The authors thank Jaehyuk Choi for making the figures and a referee for the reference to transverse jets.

REFERENCES

Bazant, M. Z. 2004 Conformal mapping of some non-harmonic functions in transport theory. *Proc. R. Soc. Lond.* A **460**, 1433–1454.

Boussinesq, M. J. 1905 Sur le pouvoir refroidissant d'un courant liquide ou gazeux. *J. de Math.* **1**, 285–290.

Burgers, J. M. 1948 A mathematical model illustrating the theory of turbulence. *Adv. Appl. Mech.* **1**, 171–199.

Choi, J., Margetis, D., Squires, T. M. & Bazant, M. Z. 2005 Steady advection–diffusion around finite absorbers in two-dimensional potential flows, *J. Fluid Mech.* **536**, 155–184.

Coelho, S. L. V. & Hunt, J. C. R. 1989 The dynamics of the near field of strong jets in crossflows. *J. Fluid Mech.* **200**, 95–120.

Cortelezzi, L. & Karagozian, A. R. 2001 On the formation of the counter-rotating vortex pair in transverse jets. *J. Fluid Mech.* **446**, 347–373.

Eames, I. & Bush, J. W. M. 1999 Long dispersion by bodies fixed in a potential flow. *Proc. R. Soc. Lond.* A **455**, 3665–3686.

Fearn, R. & Weston, R. 1974 Vorticity associated with a jet in a cross flow. *AIAA J.* **12**, 1666–1671.

Gibbon, J. D., Fokas, A. S. & Doering, C. R. 1999 Dynamically stretched vortices as solutions of the 3D Navier–Stokes equations. *Physica* D **132**, 497–510.

Hunt, J. C. R. & Eames, I. 2002 The disappearance of laminar and turbulent wakes in complex flows. *J. Fluid Mech.* **457**, 111–132.

Kamotani, Y. & Greber, I. 1972 Experiments on a turbulent jet in a cross flow. *AIAA J.* **10**, 1425–1429.

Kelso, R. M., Lim, T. T. & Perry, A. E. 1996 An experimental study of round jets in cross flow. *J. Fluid Mech.* **306**, 111–144.

Koplik, J., Redner, S. & Hinch, E. J. 1994 Tracer dispersion in planar multipole flows. *Phys. Rev.* E **50**, 4650–4667.

Kornev, K. & Mukhamadullina, G. 1994 Mathematical theory of freezing for flow in porous media. *Proc. R. Soc. Lond.* A **447**, 281–297.

Maksimov, V. A. 1976 On the determination of the shape of bodies formed by solidification of the fluid phase of the stream. *J. Appl. Math. Mech.* (*Prikl. Mat. Mekh.*) **40**, 264–272.

Muppidi, S. & Mahesh, K. 2005*a* Study of trajectories of jets in crossflow using direct numerical simulations. *J. Fluid Mech.* **530**, 81–100.

Muppidi, S. & Mahesh, K. 2005*b* Velocity field of a round turbulent transverse jet. *Fourth Intl Symp. on Turbulence and Shear Flow Phenomena, Williamsburg, VA, Paper* TSFP4-197.

Needham, T. 1997 *Visual Complex Analysis*. Clarendon.

Pearson, C. E. 1957 On the finite strip problem. *Q. Appl. Maths* **XV**, 203–208.

Smith, S. H. & Mungal, M. G. 1998 Mixing, structure and scaling of the jet in crossflow. *J. Fluid Mech.* **357**, 83–122.

Su, L. K. & Mungal, M. G. 2004 Simultaneous measurement of scalar and velocity field evolution in turbulent crossflowing jets. *J. Fluid Mech.* **513**, 1–45.

van Wijngaarden, L. 1966 Asymptotic solution of a diffusion problem with mixed boundary conditions. *Proc. Koninkl. Nederl. Akad. Wet.* **69**, 263–276.

Yuan, L. L. & Street, R. L. 1998 Trajectory and entrainment of a round jet in crossflow. *Phys. Fluids* **10**, 2323–2335.